Screening of immunosuppressive factors for biomarkers of breast cancer malignant phenotypes and subtype-specific targeted therapy

Zhuoqi Liu [Equal first author, 1], **Ping Wang** [Equal first author, 2], **Yunlei Song** [3], **Jiaxuan Liu** [2], **Qiang Liu** [4], **Chao Wang** [5], **Caiyun Qian** [1], **Shuhua Zhang** [6], **Weifeng Zhu** [1], **Xiaohong Yang** [1], **Fusheng Wan** [Corresp., 1], **Daya Luo** [Corresp. 1, 7]

[1] Department of Biochemistry and Molecular Biology, School of Basic Medical Sciences, Nanchang University, Nanchang, China

[2] Queen Mary School, Nanchang University, Nanchang, China

[3] Key Laboratory of Prevention and treatment of cardiovascular and cerebrovascular diseases of Ministry of Education, Gannan Medical University, Ganzhou, China

[4] National Cancer Center/Cancer Hospital, Chinese Academy of Medical Sciences and Peking Union Medical College, Beijing, China

[5] School of Basic Medical Sciences, Nanchang University, Nanchang, China

[6] Jiangxi Cardiovascular Research Institute, Jiangxi Provincial People's Hospital, Nanchang, China

[7] Jiangxi Province Key Laboratory of Tumor Pathogens and Molecular Pathology, Nanchang University, Nanchang, People's Republic of China

Corresponding Authors: Fusheng Wan, Daya Luo
Email address: wanfs01@163.com, luodaya@ncu.edu.cn

To screen and validate immunosuppressive factors in luminal- and basal-like breast cancer cell lines and tissue samples associated with malignant phenotypes. The mRNA microarray datasets, GSE40057 and GSE1561, were downloaded and remodelled, and differentially expressed genes (DEGs) were identified. Weighted Gene Co-expression Network Analysis (WGCNA) and Gene Ontology (GO) and KEGG pathway enrichment analysis were performed to explore the immune-related events that related to the basal-like trait. The online resources, GOBO, Kaplan-Meier Plotter and UALCAN, were employed to screen for immunosuppressive factors associated with breast cancer malignant phenotypes. Immunohistochemistry was used to evaluate *VEGFA* and *MIF* levels in breast tumours and normal breast tissues; qPCR and western blot were used to validate the expression of clinical immune-oncology (IO) therapeutic targets *CD274* (*PD-L1*) and IL8 in cell lines. The results showed that there were varies immune-related events contribute to the trait of basal-like breast cancer. First, *TGFβ1* and *IL8* have higher average expression levels in more malignant cell lines; Second, *MIF* and *VEGFA* have higher average expression levels in more malignant breast cancer tissue, and the high expression levels of them were associated with poor survival rate. Third, IO targets *CD274* and *IL8* were confirmed that more suitable for the treatment of basal-like breast cancer. In view of the above, during the formation and development of breast cancer, immune-related genes are always activated, and immunosuppressive factors, *IL8*, *TGFβ1*, *MIF* and *VEGFA* are up-regulated. Such molecules could be used as biomarkers for breast cancer prognosis . However,

because individual immune-related factors can play several biological roles, the mechanistic relationship between immunosuppressive factors and breast cancer malignant phenotypes and the feasibility of their application as drug targets require further investigation.

Introduction

Breast cancer, the most diagnosed cancer and the second most fatal malignancy in women around the world, happens to one in eight women("Cancer facts $figures 2016," 2016). With the advent of gene expression profiling over the last 15 years, breast cancers have been classified into luminal A, luminal B, human epidermal growth factor receptor 2 (HER2 or ERBB2)-enriched, basal-like, and claudin-low(Liu & Wang, 2015; Prat et al., 2015). Among these categories, basal-like breast cancer has garnered significant attention among researchers, as it accounts for ~75% of the highly malignant triple negative subtype. This biologically aggressive neoplasia takes on several malignant phenotypes, including early onset, higher histological grade, increased distant recurrence and visceral metastases, insensitivity to endocrine and targeted therapy and poor prognosis(Bahnassy et al., 2015). Although biomarkers for breast cancer prognosis and therapy(Jezequel et al., 2012) have markedly improved treatment decisions, inconsistent diagnostic criteria for basal-like breast cancer and controversial research findings necessitate the discovery of more specific molecular markers(Tomao et al., 2015).

Malignant tumour phenotypes, such as invasiveness, metastasis, drug resistance and poor prognosis, depend on both the distinct genetic and epigenetic characteristics of the tumour as well as other factors in the tumour microenvironment(Gandellini et al., 2015). The tumour microenvironment is composed of tumour cells, various types of stromal cells and the extracellular matrix, in which tumour cells and stromal cells interact by releasing a variety of cytokines, chemokines and growth factors(M. Xu et al., 2012). In the last few years, it has become obvious that tumour cells, as well as other cells and factors that accumulate in tumour-bearing hosts, play a critical role in patient outcome(Schlößer et al., 2014). On one hand, a variety of immune cells can be induced to kill tumour cells. On the other hand, tumour cells have many strategies for escaping immune attack, including the release of immunosuppressive factors. The presence of immunosuppressive factors induces local immune escape in the tumour microenvironment, which thwart anti-tumour immune responses and pose a major obstacle to many immunotherapeutic or conventional therapeutic approaches. Fortunately, the high expression of those immunosuppressive factors may also be studied as therapeutic targets. Nowadays, there are multiple immune-oncology (IO) therapeutic targets have been available in clinical therapy(Szekely et al., 2018). However, due to the multifaceted functions of many immunosuppressive factors in different tumour types and stages of development, there remains controversy regarding their true and fundamental roles in tumour pathology. This ambiguity prevents the clinical application of immunosuppressive factors as diagnostic and therapeutic biomarkers.

In this paper, by comparing gene expression patterns between basal- and luminal-like breast cancer cell lines and tissue samples, which have different levels of aggressiveness and malignancy, we attempt to screen and verify the immunosuppressive factors associated with a malignant phenotype and investigate the significance of IO targets in the clinical treatment of

breast cancer. These immunosuppressive factors could be used as additional markers to identify malignant breast cancer and further tailor therapies for individual breast cancer patients.

Materials and Methods

Gene Expression Microarray Analysis

The expression monitoring arrays raw data for were downloaded from Gene Expression Omnibus (GEO) database(Barrett et al., 2012)with accession number: GSE40057(Luo et al., 2013) and GSE1561(Farmer et al., 2005). The GSE40057 analyzed 10 breast cancer cell lines and 2 immortalized breast epithelium cell lines with the Affymetrix Human Genome U133 Plus 2.0 Array; GSE1561 contained 49 breast cancer tissue samples and were tested on Affymetrix U133A chips. Principal components analysis (PCA), K-means clustering and differentially expressed genes (DEGs) screening were performed in R using Bioconductor and associated packages(Gentleman et al., 2004).

Weighted Gene Co-expression Network Analysis (WGCNA) and Gene ontology (GO) and KEGG pathway Enrichment Analysis

For genome-wide expression profile data of tissues and cell lines, the missing value were first removed and the genes whose average expression level less than 0.5 were filtered. Secondly, all samples performed well in hierarchical clustering, and no outliers needed to be removed. Step-by-step method of WGCNA package(Langfelder & Horvath, 2008) in R was used to construct the module and co-expression network. Soft thresholds were generated by the pickSoftThreshold function of WGCNA package, with tissue data set to 28 and cell line data set to 10. Adjacency matrix and the topological overlap matrix (TOM) were calculated according to the corresponding soft threshold. Based on TOM, the corresponding dissimilarities between each gene were calculated and 400 genes were randomly selected for the visualization of TOM. At the same time, we constructed the hierarchical cluster tree of all genes based on the dissimilarity matrix. Using the dynamic tree cut method, the branches of the hierarchical cluster tree were cut to identify modules. Subsequently, with the hierarchical clustering data of module eigengene data, a height cut of 0.25 was chosen, and similar modules were merged to build the final co-expression network. Finally, the visualization of module eigengene data we performed and module-trait associations were quantified. GO and KEGG pathway enrichment analyses were performed for genes in each module using the DAVID functional annotation clustering tool (http://david.abcc.ncifcrf.gov)(Huang da, Sherman, & Lempicki, 2009)

GOBO analysis

GOBO (http://co.bmc.lu.se/gobo/), an online resource with mRNA microarray profiling data from 51 breast derived cell lines(Ringner, Fredlund, Hakkinen, Borg, & Staaf, 2011), was used to validate the mRNA expression levels of four immunosuppressive factor genes screened from cell lines of GSE40057.

UALCAN and Kaplan-Meier survival analyses

UALCAN (http://ualcan.path.uab.edu/index.html), an interactive web resource that contain large amount of cancer transcriptome data derived from TCGA and MET500 transcriptome sequencing(Chandrashekar et al., 2017), was used to explore the mRNA expression levels of 6 immunosuppressive factor genes screened from tissue samples of GSE1561 in different breast cancer subtypes and normal breast tissue. Kaplan-Meier Plotter (http://kmplot.com/analysis/), an open web-based resource(Gyorffy, Surowiak, Budczies, & Lanczky, 2013), was used to determine the relationship between survival rate and mRNA expression levels of 6 immunosuppressive factor genes screened from tissue samples of GSE1561.

Immunohistochemistry (IHC)

VEGFA and MIF levels in normal and breast cancer tissues were evaluated by IHC, which use polyclonal antibodies (1:250 dilution, DF7470 and DF6404, Affinity Biosciences, Cincinnati, USA) on commercial tissue arrays (Shanghai Outdo Biotech Co., Shanghai). The array consists of 10 normal and 90 breast tumour specimens. Each sample was given a modified histochemical score (MH-score), which is affected by both the proportion and the intensity of cells stained at each intensity, to reflect the staining intensity. The intensity of each grade is the average of MH-score of all samples in that grade.

Cell culture and total RNA isolation

Breast cancer cell lines MDA-MB-231 and T47D were cultured in DMEM media supplemented with 10% fetal bovine serum (FBS), MCF7 was cultured in RPMI-1640 Medium with 10%FBS, BT549 was cultured in RPMI-1640 Medium with 0.023 IU/ml insulin and 10%FBS. Total RNA was extracted using the TRIzol® reagent (Invitrogen, Carlsbad, CA, USA).

***q*RT-PCR analysis of mRNA expression of CD274 and IL8**

2 μg of the total RNA was reverse-transcribed using RevertAid™ First Strand cDNA Synthesis Kit (Thermo, Boston, USA). SYBR® Premix Ex Taq™II (TaKaRa, Shiga, Japan) was used to conduct quantitative RT-PCR. The primer sequences used for RT-PCR are as follows: CD274-Forward: CGTTGTGCTTGAACCCTTGA, CD274-Reverse: ACACAAGGAGCTCTGTTGGA; IL8-Forward: GAGACAGCAGAGCACACAAG, IL8-Reverse: TTGGGGTGGAAAGGTTTGGA; β-actin-Forward: GAACGGTGAAGGTGACAG, β-actin-Reverse: TAGAGAGAAGTGGGGTGG. Each sample was run in triplicate. According to the manufacturer's suggested protocols, Applied Biosystems® 7500 Real-Time PCR Systems (Thermo, Boston, USA) were used in the real time PCR reaction. ΔΔCt method was used to calculate fold change in gene expression.

Western blot analysis of protein expression of CD274 and IL8

Total proteins were extracted from cells in RIPA Lysis Buffer (Vazyme, Piscataway, NJ, USA) containing protease inhibitors. 40 μg of protein from each sample was denatured, fractionated by

10% SDS-PAGE, and transferred to PVDF membranes (Immobilon®-P Transfer Membrane, Millipore, Milan, Italy). After blocking of non-specific antigens with 5% skim milk solution, blots were incubated overnight at 4℃ with primary rabbit monoclonal antibodies against *IL8* (1:1000 working dilution, DF6998, Affinity Biosciences, Cincinnati, USA) or *CD274* (1:1000 working dilution, DF6526, Affinity Biosciences, Cincinnati, USA) or β-actin (1:1000 working dilution, Santa Cruz Biotechnology, Inc., Santa Cruz, CA, USA) in 5% skim milk 0.05% TBS-Tween 20 buffer. Antibody binding to the membrane was detected with a secondary antibody (goat anti-rabbit IgG 1:5000, ZSGB Biosciences, Beijing, China) conjugated to horseradish peroxidase and visualized by enzyme-linked chemiluminescence (EasySee® Western Blot Kit, TransGen Biotechnology, Beijing, China) with the Scientific MYECL Imager (Thermo, Boston, USA). Densitometric analysis performed with ImageJ software was to normalize the signal of *IL8* and *CD274*. The intensity of the two bands was normalized against the signal of b-actin.

Statistical analysis

Each experiment was repeated at least 3 times. DEGs were identified by Bioconductor 'limma' package using a moderated t-tests ($P<0.05$) and comparisons of multiples of change (basal vs. luminal, GSE40057>2-fold, GSE1561>1.5-fold). The association of MIF and VEGFA expression and clinico-pathological data was analyzed by one-way ANOVA in SPSS 17.0 (SPSS Inc. Chicago, IL).

Results

Identification of DEGs

To study the gene expression profiles of different breast cancer cell lines and tissue-based microarray datasets, GSE40057 and GSE1561 from the GEO database were downloaded, re-modelled, analysed and compared (Fig. 1). The results showed that the number of statistically significant DEGs between luminal-like and basal-like groups of cell lines and tissue samples were 2188 and 1963, respectively.

WGCNA and GO and KEGG pathway Enrichment analyses of each gene module

To investigate what causes the difference of malignant degree between basal-like and luminal-like breast cancer, the sets of genes related to basal- and luminal-like breast cancer were first screened by constructing a gene co-expression network by WGCNA. And then 25 and 6 gene modules for GSE40057 (cell lines) and GSE1561 (tissue samples) were identified, respectively (Fig. 2A and 2C). The member genes involved in the same module are highly interconnected and were further analyzed in GO and KEGG pathway enrichment analysis. For cell lines, module lightyellow, lightgreen, darkmagenta etc. have stronger correlation with luminal-like trait; module black, orange, royalblue etc. have stronger correlation with basal-like trait (Fig. 2B). For tissue samples, module tan has stronger correlation with luminal-like trait and module red, grey etc. have stronger correlation with basal-like trait (Fig. 2D). Interestingly, the subsequent

enrichment analyses for each module genes showed that the enrichment results of module black in tissue samples were relatively uniform in immune-related events, such as T cell costimulation, peptide antigen binding, leukocyte migration (Table 1) and Allograft rejection, Antigen processing and presentation, Graft-versus-host disease, etc. (Table 2). Genes in other modules do not show that uniform enrichment results whether in immune-related aspect or any other special aspects.

The expression of immune-related genes and immune-oncology targets

According to the Cancer Inflammation & Immunity Crosstalk PCR Array profile from Qiagen (http://www.sabiosciences.com/rt_pcr_product/HTML/PAHS-181Z.html), a total of 85 key genes (Table S1), including 16 immunosuppressive factors were enrolled for subsequent analysis. The Venn diagram (Fig. 3A) shows the intersection between immune-related genes and DEGs from GSE40057 and GSE1561; The Venn diagram (Fig. 3B) shows the intersection between 29 clinical IO targets (Table S1)(Szekely et al., 2018) and DEGs from GSE40057 and GSE1561. There are 15 immune-related genes in GSE40057 (Table S2), including 4 immunosuppressive factors, *CD274* (*PDL1*), *CSF2*, *IL8* (*CXCL8*) and *TGFβ1*; 31 immune-related genes in GSE1561 (Table S2), including 6 immunosuppressive factors, *CXCL12*, *CXCL5*, *IDO1*, *MIF*, *PTGS2* and *VEGFA*; and 6 immune-related genes in both; 2 IO targets in GSE40057, *CD274* and *IL8*; 2 IO targets in GSE1561, *CXCL12* and *IDO1*. Interestingly, compared with the luminal-like cell lines and tissue samples, most immune-related genes identified in basal-like malignancies are upregulated, except *CXCL12* (Fig. 3C and 3D).

GOBO analysis for the immunosuppressive factors screened from cell lines

GOBO analysis showed that *CSF2*, *IL8* and *TGFβ1* expression have an inconsistent expression pattern across cell lines; there is no information on GOBO for *CD274*. *IL8* have higher average expression levels in basal-like cell lines ($p<0.01$) and *TGFβ1* have higher average expression levels in basal-like and triple negative cell lines ($p<0.01$) (Fig. 4).

UALCAN and Kaplan-Meier survival analyses for the immunosuppressive factors screened from tissue

UALCAN analysis showed that only *CXCL12* has lower expression level in basal-like (triple negative) breast cancer as in comparison with luminal-like breast cancer; while *CXCL5*, *IDO1*, *MIF*, *PTGS2* and *VEGFA* all have higher expression in basal-like breast cancer (Fig. 5). Analysis of overall survival showed that higher *CXCL12*, *CXCL5*, *IDO1* and *PTGS2* mRNA expression levels were correlated with a comparatively higher survival rate ($p<0.01$), while higher *MIF* and *VEGFA* expression levels were correlated with a lower survival rate ($p<0.01$) (Fig. 6).

Expression of MIF and VEGFA in breast tissue microarrays

To validate whether MIF and VEGFA protein expression is associated with breast cancer malignancy, immunohistochemical detection was performed in tissue microarray with 90 primary tumour tissues and 10 normal breast tissue samples ($p<0.01$) (Fig. 7). The results show that MIF expression is increased dramatically in the metastasis group ($p<0.05$) and that VEGFA expression positively correlates with tumour grade ($p<0.05$) (Table 3).

CD274 (PD-L1) and IL8 are highly expressed in basal-like breast cancer cell lines

To validate the expression pattern of the two IO targets- *CD274* and *IL8*, qRT-PCR and western blot were used to detect the expression of mRNA and protein from 4 breast cancer cell lines: 2 basal-like (BT549 and MDA-MB-231) and 2 luminal-like (MCF7 and T47D)(Neve et al., 2006). qRT-PCR results (Fig. 8A) show that *CD274* and *IL8* were upregulated in the basal-like breast cancer cell lines, BT549 and MDA-MB-231 ($p<0.01$). Similar to qRT-PCR results, western blot analysis (Fig. 8B) indicates that CD274 and IL8 protein were increased in BT549 and MDA-MB-231, compared to MCF7 and T47D cell lines.

Discussion

The breast tumour microenvironment consists of epithelial tumour cells and the extracellular matrix (ECM), including stromal cells such as fibroblasts, adipocytes, endothelial and resident immune cells, a multitude of soluble factors, and more recently identified regulatory mediators, such as microRNAs, metabolites and exosomes(Dittmer & Leyh, 2015). Although cancer progression has been associated with genetic mutations and epigenetic changes in tumour cells, increasing evidence suggests that it is not entirely driven by cancer cell processes and may be influenced by the interplay between cancer cells and their surrounding microenvironment (i.e., tumour-stroma crosstalk)(Criscitiello, Esposito, & Curigliano, 2014). There is evidence demonstrating that both stroma and tumour cells evolve upon tumour initiation and progression, which makes the tumour-stroma environment distinct from that of healthy tissue(Quail & Joyce, 2013). Upon its conversion from normal stroma, tumour stroma thwarts anti-cancer activities and promotes cancer progression(Granot & Fridlender, 2015). Based on the aforementioned reasons, the molecular changes in tumour cells often do not reflect all the changes that occur during tumour-stroma crosstalk in the microenvironment(Morandi & Chiarugi, 2014).

In this paper, 2 original datasets, GSE40057 and GSE1561, were downloaded from the GEO database. To avoid the inaccuracy produced by ‘edged’ samples, only 8 cell lines from GSE40057 and 32 tissue samples from GSE1561, representing basal-like and luminal-like groups were chosen for subsequent analyses due to their great difference in malignant degree. In the WGCNA, all genes of the microarray were assigned into corresponding modules based on the weighted gene co-expression network, and the correlations of each module with luminal and basal trait were calculated. Genes involved in the same module are highly interconnected and relate to a specific trait, which different from DEGs that only show us the differences in expression levels between groups. Therefore, we chose WGCNA analysis instead of conventional differential expression gene analysis to screen biological characteristics related to

malignant phenotype of breast cancer. GO and KEGG pathway enrichment analyses for each module showed that genes in module black of tissue samples were uniformly enriched in immune-related events, and this module obviously showed a closer correlation with basal-like rather the luminal-like breast cancer, indicating that there are some immune-related events may play pivotal role in the malignant phenotype of basal-like breast cancer. However, the enrichment results of modules in cell lines not obviously relate to immune-related events. This may because of the tumour-stroma crosstalk in vivo, which is not included in cell lines. Therefore, in the field of tumour immune research, the selection of model cell lines or tissue samples may lead to different results, and both of them have their own unique advantages in scientific research.

Tumour cells have many strategies for avoiding immune attack, including decreased tumour antigen expression by HLA molecules on the tumour cell surface, downregulation of tumour antigen presentation by dendritic cells, release of immunosuppressive factors and activation of regulatory T cells(Raposo, Beirão, Pang, Queiroga, & Argyle, 2015). Among them, the release of immunosuppressive factors to induce immunosuppression is an important mechanism for tumour cell evasion of immune surveillance(Jiang & Shapiro, 2014). Immunosuppression is a reduction of the activation or efficacy of the immune system(Schlößer et al., 2014). Both tumour cells and stromal cells can be induced to synthesize and/or secret immunosuppressive factors to evade immune surveillance, contributing to tumour initiation and progression(Grivennikov, Greten, & Karin, 2010). To date, more than 20 immunosuppressive factors produced by tumour and/or stromal cells have been discovered, including transforming growth factor-β1 (TGFβ1)(Y. Wang, Wang, Wang, Zhang, & Jiang, 2015), prostaglandin E2 (PGE2)(Kalinski, 2012), vascular endothelial growth factor (VEGF)(Shibuya, 2013), interleukin-10 (IL-10)(Geginat et al., 2016), interleukin-4 (IL-4)(Egawa et al., 2013), cyclooxygenase-2 (COX-2)(H. Li et al., 2013), programmed cell death 1 (PDCD1)(Gatalica et al., 2014) and cytotoxic T-lymphocyte associated antigen 4 (CTLA4), etc(Lan et al., 2013). Although therapeutic agents that target immunosuppressive factors, such as BMS-936559, Pidilizumab and Ipilimumab, have achieved breakthrough responses in cancer immunotherapy and represent one of the most promising strategies for tumour treatment(Schlößer et al., 2014), other immunosuppressive targets are still under investigation, as their roles in tumour malignancy are not completely understood.

Analysis of cell lines showed that *CD274*, *CSF2*, *IL8* and *TGFβ1* were up-regulated in basal-like cells lines as compared with luminal-like cell lines. Further, GOBO analysis confirmed that *IL8* and *TGFβ1* have higher average expression levels in basal-like and triple negative cell lines, indicating that *IL8* and *TGFβ1* may be associated with malignant phenotype. Analysis of tissue samples revealed that *CXCL5*, *IDO1*, *PTGS2*, *MIF* and *VEGFA* were up-regulated in basal-like tissues as compared with luminal-like tissues, which also confirmed by UALCAN analysis. Besides, Kaplan-Meier survival analysis showed that breast cancer patients with higher *MIF* and *VEGFA* expression levels were correlated with a lower survival rate. These suggest that the higher expression levels of *MIF* and *VEGFA* contribute to the malignant phenotype of breast cancer. Our results of IHC also validated it.

Cancer-derived IL8 may result in the recruitment and activation of tumour-associated neutrophils (TAN) and myeloid-derived suppressor cells (MDSCs) to contribute to the tumour microenvironment and immune suppression, and also activate endothelial cells for angiogenesis(Waugh & Wilson, 2008). IL8 functions by activating PI3K-Akt and PLC-PKC signaling pathways, respectively. These two signaling pathways have been demonstrated associated with angiogenesis, cell survival, and migration(Cheng et al., 2008). Over-expressed IL8 is associated with an accelerated breast cancer progression, a higher tumour load, and the presence of distant metastasis, ultimately leading to poor survival(Singh, Simoes, Howell, Farnie, & Clarke, 2013). TGFβ1 is a well-known family involved in various tumour progressions, such as induction of epithelial–mesenchymal transition, mediation of cancer migration and invasion(J. Xu, Lamouille, & Derynck, 2009). Over-expression of MIF has been demonstrated in multiple cancers progression, such as ovarian cancer(Krockenberger et al., 2012), hepatocellular carcinoma(D. Wang et al., 2014), gastric cancer(He et al., 2006) and other malignant cancers . Several literatures have elucidated the multiple roles of MIF in breast cancer microenvironment, including increasing the recruitment of immune suppressive cells(Simpson, Templeton, & Cross, 2012), promoting angiogenesis and breast cancer cell trans-endothelial migration(Martinez et al., 2014). In addition, MIF also acts on tumour cells to facilitate cell proliferation and cell survival(Lue et al., 2007). Thus far, VEGFA protein has been elucidated as a major factor that contribute to the tumour angiogenesis and malignant progression in variety of cancers(Q. Li et al., 2017; Yang, Xiong, Zuo, Liu, & Zhang, 2018). In recent years, there are amount of anti-angiogenic drugs has been designed and showed significant effects in chemotherapy. Unfortunately, some of these drugs (e.g. Bevacizumab) showed limited effects in specific breast cancer conditions(Bergh et al., 2012; Varinska, Gal, Mojzisova, Mirossay, & Mojzis, 2015). Therefore, patients need to be evaluated before the implementing of anti-angiogenic therapy. Prospectively, VEGFA may act as a evaluation factor to identify the breast cancer patients who might benefit from anti-angiogenic therapy.

Thus far, a range of IO targets have been available in clinical therapy(Szekely et al., 2018). Among our results, *CD274*, *IL8*, *CXCL12* and *IDO1* (Fig. 3B) are included in these IO targets. Since the Kaplan-Meier survival analysis showed that CXCL12 and IDO1 were not associated with the malignant phenotype of breast cancer, they did not studied by further experience. While high expression levels of *CD274* and *IL8* in basal-like breast cancer were validated by qRT-PCR and western blot, suggesting that clinical *CD274* and *IL8* target therapies may be more suitable for basal-like breast cancer. Other immunosuppressive factors in this study are also worth further studying in the field of subtype-specific IO target therapy for breast cancer in the future.

Conclusions

Through the use of online databases, model reconstruction and comparisons of the mRNA expression profiles of luminal-like and basal-like cell lines and primary breast cancer tissues, 4 immunosuppressive factors associated with a malignant phenotype in breast cancer were identified and validated. Such molecules could be used as biomarkers for breast cancer malignant

phenotypes and prognosis. In addition, 2 immunosuppressive factors were confirmed as clinical IO therapeutic targets, and they may more suitable for the therapy of basal-like breast cancer. However, because the majority of immune-related factors have diverse roles in disease pathology and we still lack a complete understanding of the relationship between immunosuppressive factors and breast cancer malignancy, therefore, the feasibility of their clinical application as drug targets and prognosis predictors warrants further investigation.

Acknowledgments: The authors would like to thank Ping Zhang, Qingmei Zhong, Xianhe Yang, Wu Wang, Di Yao and Yingqun Xiao at Department of Pathology, Affiliated Infectious Diseases Hospital, Nanchang University, for their technical assistance.

Funding: This work was partially supported by National Natural Science Foundation of China (No. 81160248, 81360313, 81560464) (to Daya Luo and Zhuoqi Liu), Natural Science Foundation of Jiangxi Province (No. 20151BAB205058, 20171BAB205055) (to Daya Luo and Zhuoqi Liu), Innovation Foundation for Graduate Students of Nanchang University (No. CX2015181) (to Yunlei Song). The funders had no role in study design, data collection and analysis, decision to publish, or preparation of the manuscript.

Author Contributions: DY.L. and FS.W. designed the experiments and reviewed paper; ZQ.L. , P.W. and YL.S. performed the datasets analysis and wrote the manuscript; CY.Q. , SH.Z. , WF.Z. and XH.Y. administered the cells models, qRT-PCR, Western Blot and Immunohistochemistry; JX.L. , Q.L. and C.W. executed the WGCNA analysis. All authors reviewed and approved the final version.

Conflicts of Interest: The authors declare no conflict of interest.

References

Bahnassy, A., Mohanad, M., Ismail, M. F., Shaarawy, S., El-Bastawisy, A., & Zekri, A.-R. N. (2015). Molecular biomarkers for prediction of response to treatment and survival in triple negative breast cancer patients from Egypt. *Experimental and Molecular Pathology, 99*(2), 303-311. doi: 10.1016/j.yexmp.2015.07.014

Barrett, T., Wilhite, S. E., Ledoux, P., Evangelista, C., Kim, I. F., Tomashevsky, M., . . . Soboleva, A. (2012). NCBI GEO: archive for functional genomics data sets--update. *Nucleic Acids Res, 41*(D1), D991-D995. doi: 10.1093/nar/gks1193

Bergh, J., Mariani, G., Cardoso, F., Liljegren, A., Awada, A., Vigano, L., . . . Gianni, L. (2012). Clinical and pharmacokinetic study of sunitinib and docetaxel in women with advanced breast cancer. *Breast, 21*(4), 507-513. doi: 10.1016/j.breast.2012.01.012

Cancer facts $figures 2016. (2016).

Chandrashekar, D. S., Bashel, B., Balasubramanya, S. A. H., Creighton, C. J., Ponce-Rodriguez, I., Chakravarthi, B. V., & Varambally, S. (2017). UALCAN: A Portal for Facilitating Tumor Subgroup Gene Expression and Survival Analyses1. *Neoplasia, 19*(8), 649-658. doi: 10.1016/j.neo.2017.05.002

Cheng, G. Z., Park, S., Shu, S., He, L., Kong, W., Zhang, W., . . . Cheng, J. Q. (2008). Advances of AKT pathway in human oncogenesis and as a target for anti-cancer drug discovery. *Curr Cancer Drug Targets, 8*(1), 2-6.

Criscitiello, C., Esposito, A., & Curigliano, G. (2014). Tumor–stroma crosstalk. *Current Opinion in Oncology, 26*(6), 551-555. doi: 10.1097/cco.0000000000000122

Dittmer, J., & Leyh, B. (2015). The impact of tumor stroma on drug response in breast cancer. *Semin Cancer Biol, 31*, 3-15. doi: 10.1016/j.semcancer.2014.05.006

Egawa, M., Mukai, K., Yoshikawa, S., Iki, M., Mukaida, N., Kawano, Y., . . . Karasuyama, H. (2013). Inflammatory monocytes recruited to allergic skin acquire an anti-inflammatory M2 phenotype via basophil-derived interleukin-4. *Immunity, 38*(3), 570-580.

Farmer, P., Bonnefoi, H., Becette, V., Tubiana-Hulin, M., Fumoleau, P., Larsimont, D., . . . Iggo, R. (2005). Identification of molecular apocrine breast tumours by microarray analysis. *Oncogene, 24*(29), 4660-4671. doi: 10.1038/sj.onc.1208561

Gandellini, P., Andriani, F., Merlino, G., D'Aiuto, F., Roz, L., & Callari, M. (2015). Complexity in the tumour microenvironment: Cancer associated fibroblast gene expression patterns identify both common and unique features of tumour-stroma crosstalk across cancer types. *Semin Cancer Biol, 35*, 96-106. doi: 10.1016/j.semcancer.2015.08.008

Gatalica, Z., Snyder, C., Maney, T., Ghazalpour, A., Holterman, D. A., Xiao, N., . . . Vranic, S. (2014). Programmed cell death 1 (PD-1) and its ligand (PD-L1) in common cancers and their correlation with molecular cancer type. *Cancer Epidemiology Biomarkers & Prevention, 23*(12), 2965-2970.

Geginat, J., Larghi, P., Paroni, M., Nizzoli, G., Penatti, A., Pagani, M., . . . Flavell, R. A. (2016). The light and the dark sides of Interleukin-10 in immune-mediated diseases and cancer. *Cytokine & Growth Factor Reviews*.

Gentleman, R. C., Carey, V. J., Bates, D. M., Bolstad, B., Dettling, M., Dudoit, S., . . . Zhang, J. (2004). Bioconductor: open software development for computational biology and bioinformatics. *Genome biology, 5*(10), R80. doi: 10.1186/gb-2004-5-10-r80

Granot, Z., & Fridlender, Z. G. (2015). Plasticity beyond Cancer Cells and the "Immunosuppressive Switch". *Cancer Research, 75*(21), 4441-4445. doi: 10.1158/0008-5472.can-15-1502

Grivennikov, S. I., Greten, F. R., & Karin, M. (2010). Immunity, inflammation, and cancer. *Cell, 140*(6), 883-899. doi: 10.1016/j.cell.2010.01.025

Gyorffy, B., Surowiak, P., Budczies, J., & Lanczky, A. (2013). Online survival analysis software to assess the prognostic value of biomarkers using transcriptomic data in non-small-cell lung cancer. *PLoS One, 8*(12), e82241. doi: 10.1371/journal.pone.0082241

He, X. X., Yang, J., Ding, Y. W., Liu, W., Shen, Q. Y., & Xia, H. H. (2006). Increased epithelial and serum expression of macrophage migration inhibitory factor (MIF) in gastric cancer: potential role of MIF in gastric carcinogenesis. *Gut, 55*(6), 797-802. doi: 10.1136/gut.2005.078113

Huang da, W., Sherman, B. T., & Lempicki, R. A. (2009). Systematic and integrative analysis of large gene lists using DAVID bioinformatics resources. *Nat Protoc, 4*(1), 44-57. doi: 10.1038/nprot.2008.211

Jezequel, P., Campone, M., Gouraud, W., Guerin-Charbonnel, C., Leux, C., Ricolleau, G., & Campion, L. (2012). bc-GenExMiner: an easy-to-use online platform for gene prognostic analyses in breast cancer. *Breast Cancer Res Treat, 131*(3), 765-775. doi: 10.1007/s10549-011-1457-7

Jiang, X., & Shapiro, D. J. (2014). The immune system and inflammation in breast cancer. *Molecular and Cellular Endocrinology, 382*(1), 673-682. doi: 10.1016/j.mce.2013.06.003

Kalinski, P. (2012). Regulation of immune responses by prostaglandin E2. *The Journal of Immunology, 188*(1), 21-28.

Krockenberger, M., Kranke, P., Hausler, S., Engel, J. B., Horn, E., Nurnberger, K., . . . Honig, A. (2012). Macrophage migration-inhibitory factor levels in serum of patients with ovarian cancer correlates with poor prognosis. *Anticancer Res, 32*(12), 5233-5238.

Lan, K.-H., Liu, Y.-C., Shih, Y.-S., Tsaid, C.-L., Yen, S.-H., & Lan, K.-L. (2013). A DNA vaccine against cytotoxic T-lymphocyte associated antigen-4 (CTLA-4) prevents tumor growth. *Biochem Biophys Res Commun, 440*(2), 222-228.

Langfelder, P., & Horvath, S. (2008). WGCNA: an R package for weighted correlation network analysis. *BMC Bioinformatics, 9*, 559. doi: 10.1186/1471-2105-9-559

Li, H., Edin, M. L., Bradbury, J. A., Graves, J. P., DeGraff, L. M., Gruzdev, A., . . . Bortner, C. D. (2013). Cyclooxygenase-2 inhibits T helper cell type 9 differentiation during allergic lung inflammation via down-regulation of IL-17RB. *American journal of respiratory and critical care medicine, 187*(8), 812-822.

Li, Q., Kan, X., Yin, J., Sun, L., Wang, Y., Li, Y., . . . Zhu, X. (2017). Chamaejasmine B Induces the Anergy of Vascular Endothelial Cells to VEGFA Pro-angiogenic Signal by

Autophagic Regulation of VEGFR2 in Breast Cancer. *Front Pharmacol, 8*, 963. doi: 10.3389/fphar.2017.00963

Liu, X., & Wang, Q. (2015). Screening of feature genes in distinguishing different types of breast cancer using support vector machine. *OncoTargets and Therapy*, 2311. doi: 10.2147/ott.s85271

Lue, H., Thiele, M., Franz, J., Dahl, E., Speckgens, S., Leng, L., . . . Bernhagen, J. (2007). Macrophage migration inhibitory factor (MIF) promotes cell survival by activation of the Akt pathway and role for CSN5/JAB1 in the control of autocrine MIF activity. *Oncogene, 26*(35), 5046-5059. doi: 10.1038/sj.onc.1210318

Luo, D., Wilson, J. M., Harvel, N., Liu, J., Pei, L., Huang, S., . . . Shi, H. (2013). A systematic evaluation of miRNA:mRNA interactions involved in the migration and invasion of breast cancer cells. *J Transl Med, 11*(1), 57. doi: 10.1186/1479-5876-11-57

Martinez, L. M., Vallone, V. B., Labovsky, V., Choi, H., Hofer, E. L., Feldman, L., . . . Chasseing, N. A. (2014). Changes in the peripheral blood and bone marrow from untreated advanced breast cancer patients that are associated with the establishment of bone metastases. *Clin Exp Metastasis, 31*(2), 213-232. doi: 10.1007/s10585-013-9622-5

Morandi, A., & Chiarugi, P. (2014). Metabolic implication of tumor:stroma crosstalk in breast cancer. *Journal of Molecular Medicine, 92*(2), 117-126. doi: 10.1007/s00109-014-1124-7

Neve, R. M., Chin, K., Fridlyand, J., Yeh, J., Baehner, F. L., Fevr, T., . . . Gray, J. W. (2006). A collection of breast cancer cell lines for the study of functionally distinct cancer subtypes. *Cancer Cell, 10*(6), 515-527. doi: 10.1016/j.ccr.2006.10.008

Prat, A., Pineda, E., Adamo, B., Galvan, P., Fernandez, A., Gaba, L., . . . Munoz, M. (2015). Clinical implications of the intrinsic molecular subtypes of breast cancer. *Breast, 24 Suppl 2*, S26-35. doi: 10.1016/j.breast.2015.07.008

Quail, D. F., & Joyce, J. A. (2013). Microenvironmental regulation of tumor progression and metastasis. *Nature medicine, 19*(11), 1423-1437. doi: 10.1038/nm.3394

Raposo, T. P., Beirão, B. C. B., Pang, L. Y., Queiroga, F. L., & Argyle, D. J. (2015). Inflammation and cancer: Till death tears them apart. *The Veterinary Journal, 205*(2), 161-174. doi: 10.1016/j.tvjl.2015.04.015

Ringner, M., Fredlund, E., Hakkinen, J., Borg, A., & Staaf, J. (2011). GOBO: gene expression-based outcome for breast cancer online. *PLoS One, 6*(3), e17911. doi: 10.1371/journal.pone.0017911

Schlößer, H. A., Theurich, S., Shimabukuro-Vornhagen, A., Holtick, U., Stippel, D. L., & Bergwelt-Baildon, M. v. (2014). Overcoming tumor-mediated immunosuppression. *Immunotherapy, 6*(9), 973-988. doi: 10.2217/imt.14.58

Shibuya, M. (2013). Vascular endothelial growth factor and its receptor system: physiological functions in angiogenesis and pathological roles in various diseases. *Journal of biochemistry, 153*(1), 13-19.

Simpson, K. D., Templeton, D. J., & Cross, J. V. (2012). Macrophage migration inhibitory factor promotes tumor growth and metastasis by inducing myeloid-derived suppressor cells in the tumor microenvironment. *J Immunol, 189*(12), 5533-5540. doi: 10.4049/jimmunol.1201161

Singh, J. K., Simoes, B. M., Howell, S. J., Farnie, G., & Clarke, R. B. (2013). Recent advances reveal IL-8 signaling as a potential key to targeting breast cancer stem cells. *Breast Cancer Res, 15*(4), 210. doi: 10.1186/bcr3436

Szekely, B., Bossuyt, V., Li, X., Wali, V. B., Patwardhan, G. A., Frederick, C., . . . Pusztai, L. (2018). Immunological differences between primary and metastatic breast cancer. *Ann Oncol*. doi: 10.1093/annonc/mdy399

Tomao, S., Tomao, F., Rossi, L., Zaccarelli, E., Caruso, D., Minozzi, M., . . . Vici. (2015). Triple-negative breast cancer: new perspectives for targeted therapies. *OncoTargets and Therapy*, 177. doi: 10.2147/ott.s67673

Varinska, L., Gal, P., Mojzisova, G., Mirossay, L., & Mojzis, J. (2015). Soy and breast cancer: focus on angiogenesis. *Int J Mol Sci, 16*(5), 11728-11749. doi: 10.3390/ijms160511728

Wang, D., Luo, L., Chen, W., Chen, L. Z., Zeng, W. T., Li, W., & Huang, X. H. (2014). Significance of the vascular endothelial growth factor and the macrophage migration inhibitory factor in the progression of hepatocellular carcinoma. *Oncol Rep, 31*(3), 1199-1204. doi: 10.3892/or.2013.2946

Wang, Y., Wang, X., Wang, X., Zhang, D., & Jiang, S. (2015). Effect of transforming growth factor-beta1 869C/T polymorphism and radiation pneumonitis. *Int J Clin Exp Pathol, 8*(3), 2835-2839.

Waugh, D. J., & Wilson, C. (2008). The interleukin-8 pathway in cancer. *Clin Cancer Res, 14*(21), 6735-6741. doi: 10.1158/1078-0432.ccr-07-4843

Xu, J., Lamouille, S., & Derynck, R. (2009). TGF-beta-induced epithelial to mesenchymal transition. *Cell Res, 19*(2), 156-172. doi: 10.1038/cr.2009.5

466 Xu, M., Du, X., Liu, M., Li, S., Li, X., Fu, Y.-X., & Wang, S. (2012). The tumor
467 immunosuppressive microenvironment impairs the therapy of anti-HER2/neu antibody.
468 *Protein Cell, 3*(6), 441-449. doi: 10.1007/s13238-012-2044-3
469 Yang, P., Xiong, J., Zuo, L., Liu, K., & Zhang, H. (2018). miR1405p regulates cell migration
470 and invasion of nonsmall cell lung cancer cells through targeting VEGFA. *Mol Med Rep*.
471 doi: 10.3892/mmr.2018.9291

472

Figure 1

Unsupervised analysis.

(A) Principal components of all genes. The first two PCA are plotted. The three major groups were colored in blue (basal-like), red (luminal-like) and green (edged samples). (B) Hierarchical clustering of all samples. 8 cell lines from GSE40057 and 32 tissue samples from GSE1561, representing basal-like (blue) and luminal-like (red) groups were chosen for subsequent analysis.

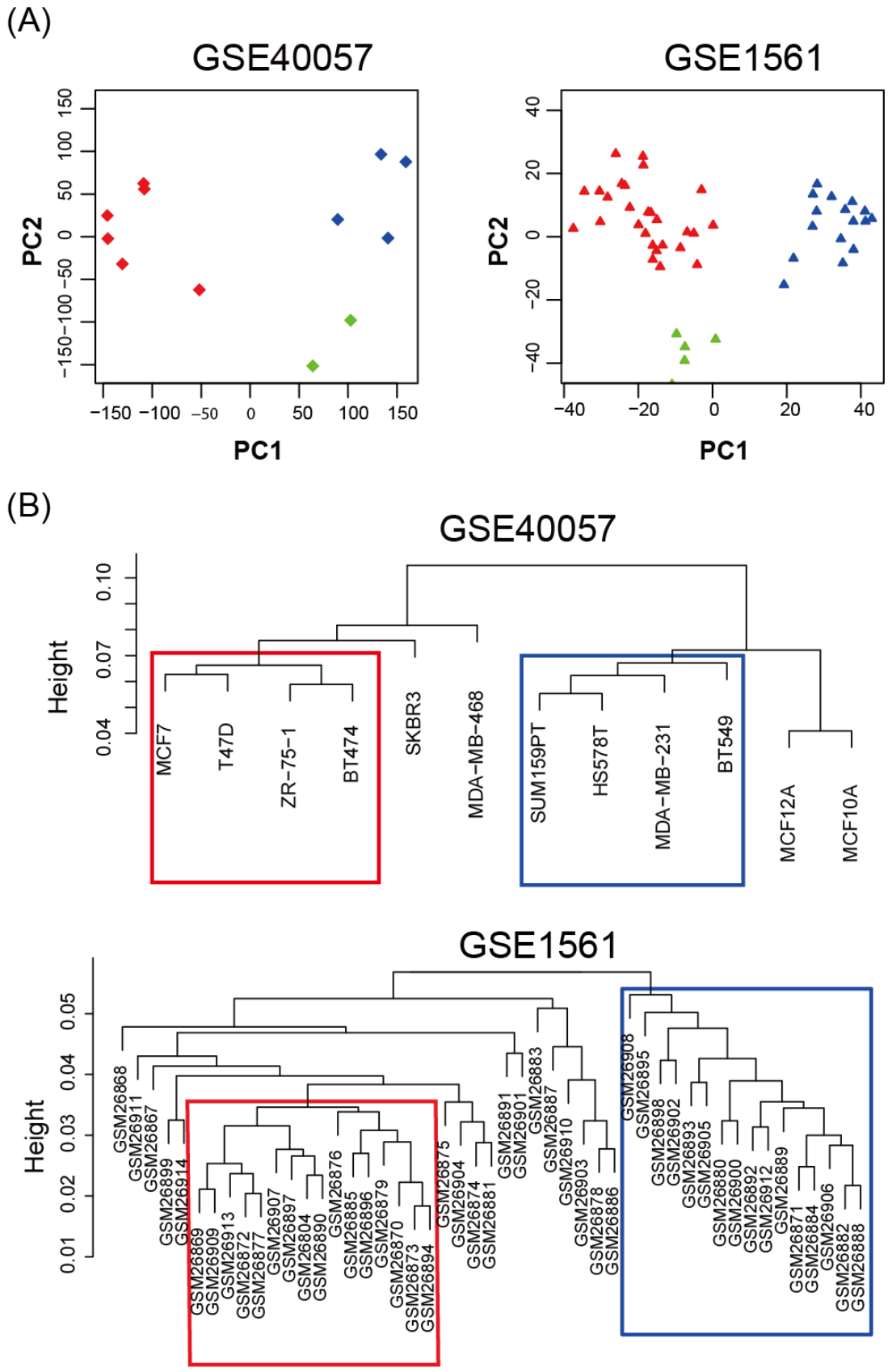
(A)
GSE40057
PC2
PC1
GSE1561
PC2
PC1
(B)
GSE40057
Height
MCF7
T47D
ZR−75−1
BT474
SKBR3
MDA−MB−468
SUM159PT
HS578T
MDA−MB−231
BT549
MCF12A
MCF10A
GSE1561
Height

Figure 2

WGCNA of GSE40057 (A, B) and GSE1561 (C, D).

(A) 20283 genes were assigned to 25 modules. The gene dendrogram was shown in the top portion, and the 25 gene modules were in the bottom portion. (B, D) Relationship between modules and traits. The upper score in each box represents module significance (MS) score, the larger the score, the higher the correlation between module and trait, and the lower value represents the corresponding p-value. (C) 12752 genes were assigned to 6 modules.

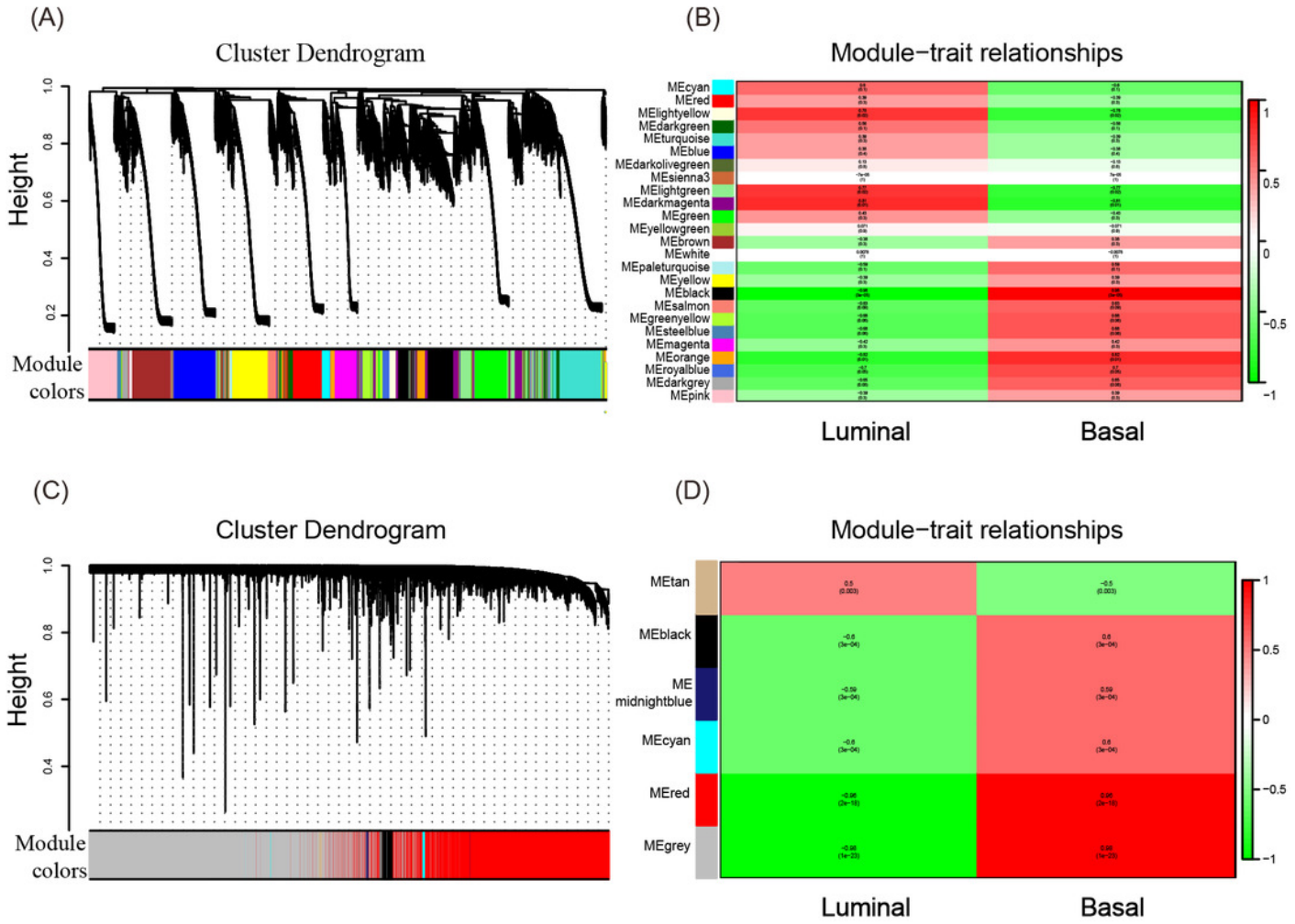

Figure 3

The expression of immune-related genes in cell lines and tissue samples.

(A) The Venn diagram shows the intersection between immune-related genes and DEGs from GSE40057 and GSE1561. (B) The Venn diagram shows the intersection between 29 clinical IO therapeutic targets and DEGs from GSE40057 and GSE1561: CD274 and IL8 from GSE40047; CXCL12 and IDO1 from GSE1561. (C, D) Hierarchical clustering analysis of Immune-related genes expression in Cell lines (C) and Tissue samples (D). Each row corresponds to an Immune-related genes and each column corresponds to an independent cell or tissue sample. The darker colour means a higher expression and the immune-related genes in red letters are thought to be immunosuppressive factors. * = IO target

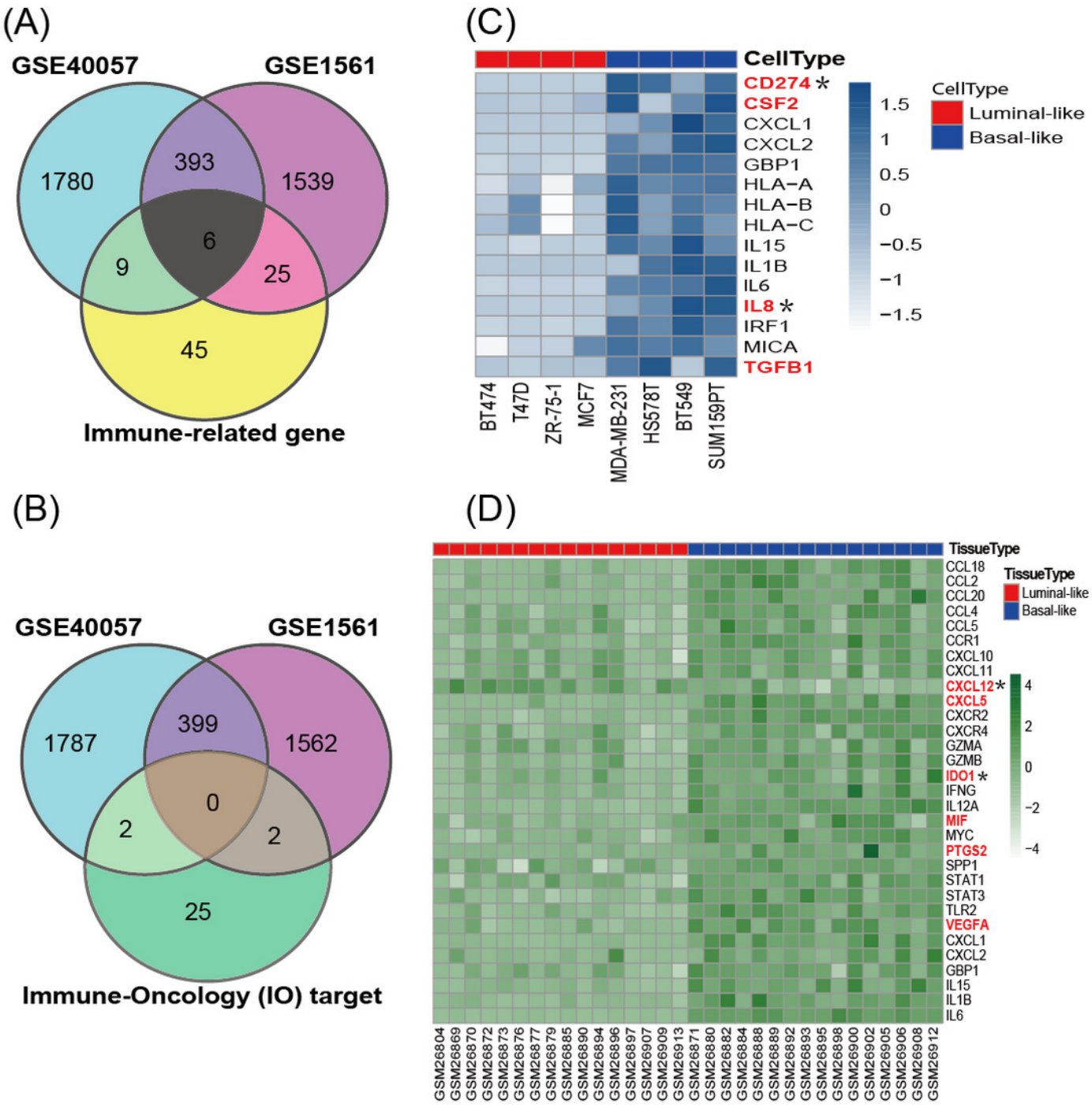
(A)
GSE40057
GSE1561
1780
393
1539
6
9
25
45
Immune-related gene
(B)
GSE40057
GSE1561
1787
399
1562
0
2
2
25
Immune-Oncology (IO) target
(C)
CellType
CD274 *
CSF2
CXCL1
CXCL2
GBP1
HLA−A
HLA−B
HLA−C
IL15
IL1B
IL6
IL8 *
IRF1
MICA
TGFB1
1.5
1
0.5
0
−0.5
−1
−1.5
CellType
Luminal-like
Basal-like
BT474
T47D
ZR-75-1
MCF7
MDA-MB-231
HS578T
BT549
SUM159PT
(D)
TissueType
CCL18
CCL2
CCL20
CCL4
CCL5
CCR1
CXCL10
CXCL11
CXCL12 *
CXCL5
CXCR2
CXCR4
GZMA
GZMB
IDO1 *
IFNG
IL12A
MIF
MYC
PTGS2
SPP1
STAT1
STAT3
TLR2
VEGFA
CXCL1
CXCL2
GBP1
IL15
IL1B
IL6
TissueType
Luminal-like
Basal-like
4
2
0
−2
−4
GSM26804
GSM26869
GSM26870
GSM26872
GSM26873
GSM26876
GSM26877
GSM26879
GSM26885
GSM26890
GSM26894
GSM26896
GSM26897
GSM26907
GSM26909
GSM26913
GSM26871
GSM26880
GSM26882
GSM26884
GSM26888
GSM26889
GSM26892
GSM26893
GSM26895
GSM26898
GSM26900
GSM26902
GSM26905
GSM26906
GSM26908
GSM26912

Figure 4

CSF2, IL8 and TGFβ1 expression in human breast cancer cell lines with GOBO analysis.

(A) Box plots of CSF2, IL8 and TGFβ1 expression across 51 breast cancer cell lines grouped into basal A (red), basal B (grey) and luminal (blue) subgroups. (B) Box plots of CSF2, IL8 and TGFβ1 expression across 51 breast cancer cell lines grouped into triple negative (TN), HER2 positive and hormone receptor positive (HR). (C) CSF2, IL8 and TGFβ1 mRNA levels across 51 breast cancer cell lines.

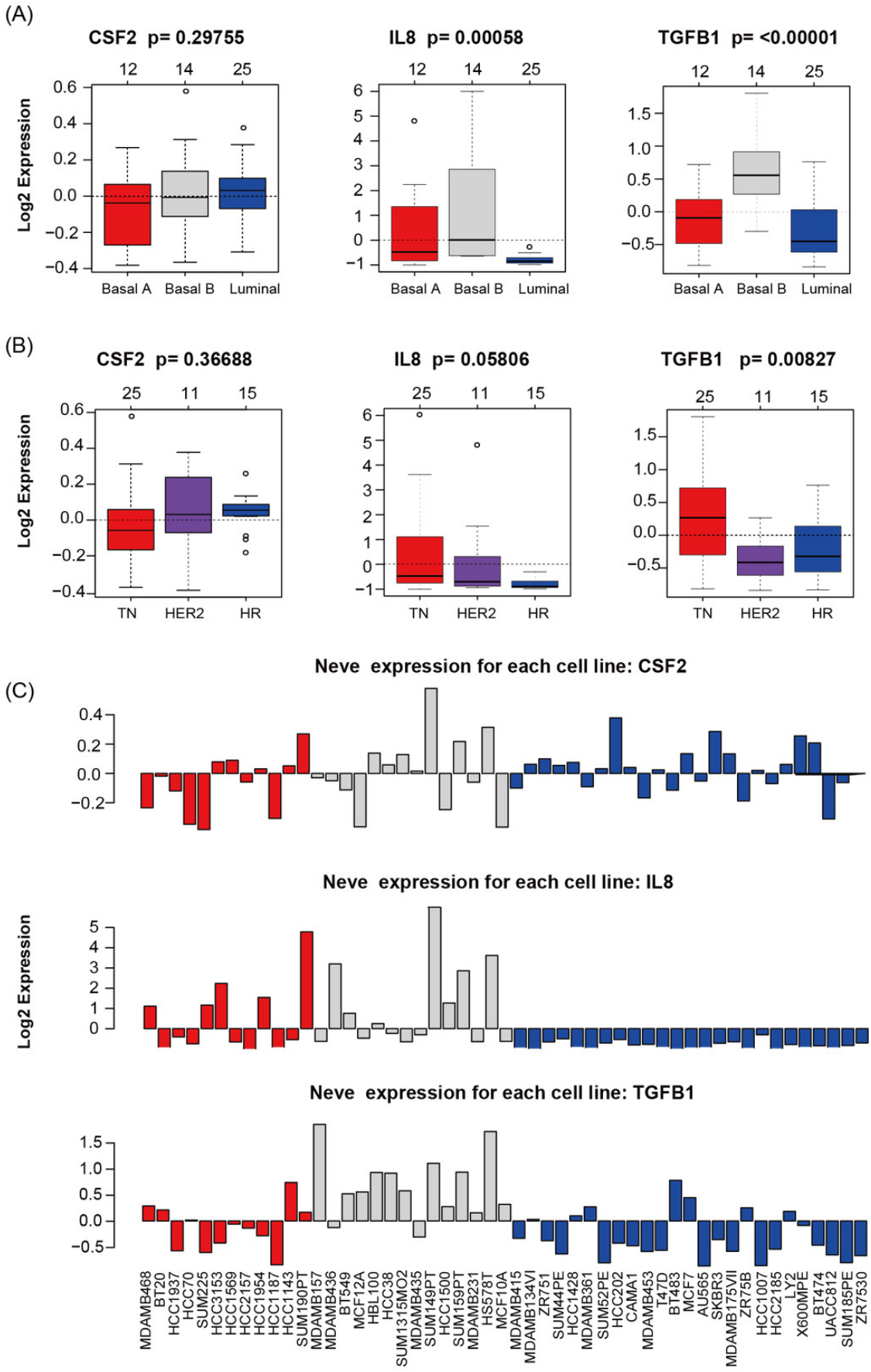
(A)
CSF2 p= 0.29755
IL8 p= 0.00058
TGFB1 p= <0.00001
Log2 Expression
12 14 25
Basal A Basal B Luminal
(B)
CSF2 p= 0.36688
IL8 p= 0.05806
TGFB1 p= 0.00827
25 11 15
TN HER2 HR
(C)
Neve expression for each cell line: CSF2
Neve expression for each cell line: IL8
Neve expression for each cell line: TGFB1
MDAMB468 BT20 HCC1937 HCC70 SUM225 HCC3153 HCC1569 HCC2157 HCC1954 HCC1187 HCC1143 SUM190PT MDAMB157 MDAMB436 BT549 MCF12A HBL100 HCC38 SUM1315MO2 MDAMB435 SUM149PT HCC1500 SUM159PT MDAMB231 HS578T MCF10A MDAMB415 MDAMB134VI ZR751 SUM44PE HCC1428 MDAMB361 SUM52PE HCC202 CAMA1 MDAMB453 T47D BT483 MCF7 AU565 SKBR3 MDAMB175VII ZR75B HCC1007 HCC2185 LY2 X600MPE BT474 UACC812 SUM185PE ZR7530

Figure 5

Expression of the six immuosuppressive factors in breast cancer based on breast cancer subtypes.

CXCL5, IDO1, MIF, PTGS2 and VEGFA have higher expression in basal (triple negative) breast cancer as compared with luminal breast cancer, while CXCL12 has lower expression in basal (triple negative) breast cancer. *p<0.05, **p<0.005, ***p<0.001.

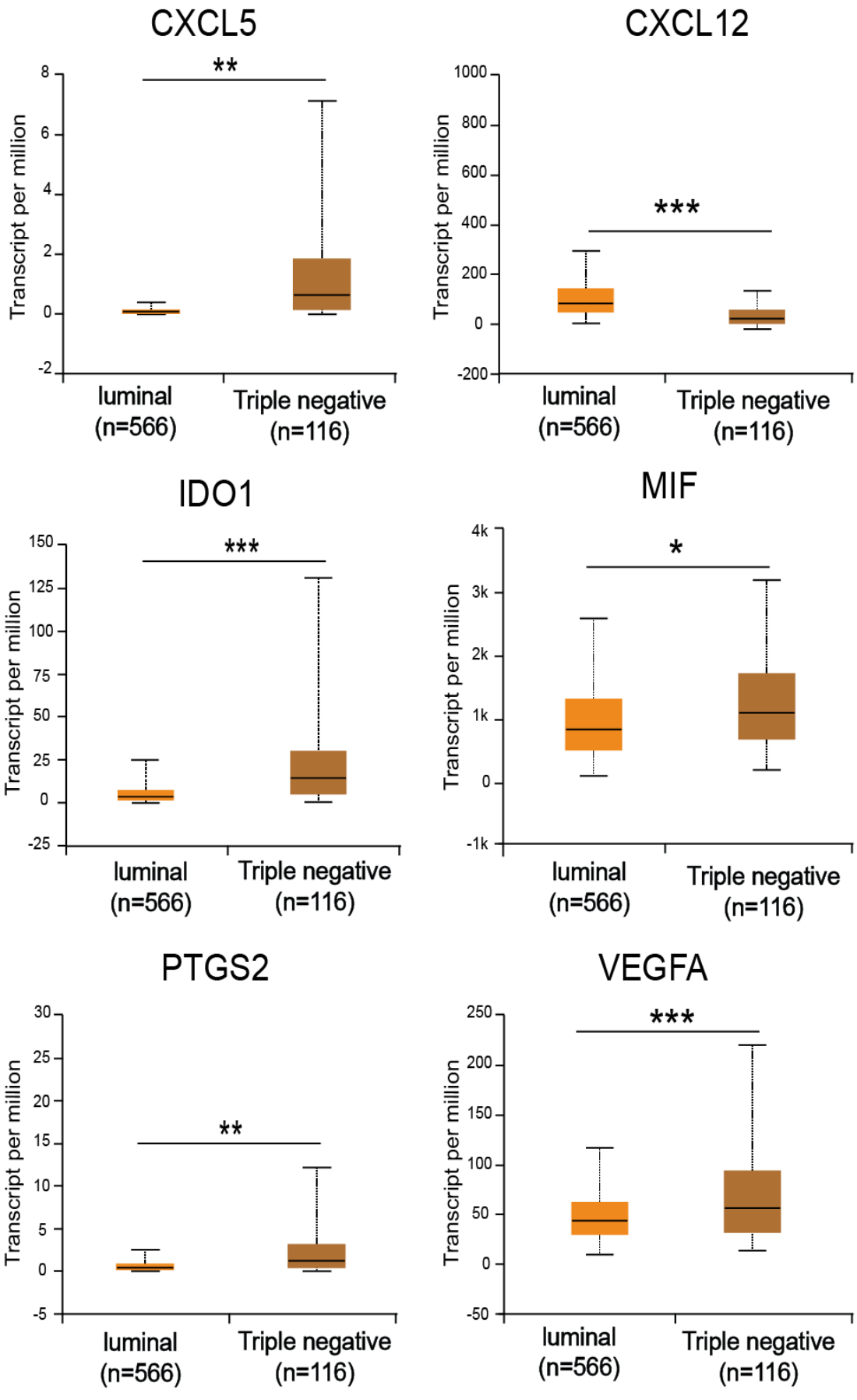
CXCL5
**
Transcript per million
8
6
4
2
0
-2
luminal (n=566)
Triple negative (n=116)
CXCL12
***
Transcript per million
1000
800
600
400
200
0
-200
luminal (n=566)
Triple negative (n=116)
IDO1
***
Transcript per million
150
125
100
75
50
25
0
-25
luminal (n=566)
Triple negative (n=116)
MIF
*
Transcript per million
4k
3k
2k
1k
0
-1k
luminal (n=566)
Triple negative (n=116)
PTGS2
**
Transcript per million
30
25
20
15
10
5
0
-5
luminal (n=566)
Triple negative (n=116)
VEGFA
***
Transcript per million
250
200
150
100
50
0
-50
luminal (n=566)
Triple negative (n=116)

Figure 6

Kaplan-Meier Plotter determined the relationship between survival rate and mRNA expression levels of 6 immunosuppressive factors using microarray data of 3951 patients.

Higher CXCL12, CXCL5, IDO1 and PTGS2 mRNA expression levels were correlated with a comparatively higher survival rate ($p<0.01$), while higher MIF and VEGFA expression levels were correlated with a lower survival rate ($p<0.01$). HR=Hazard Ratio

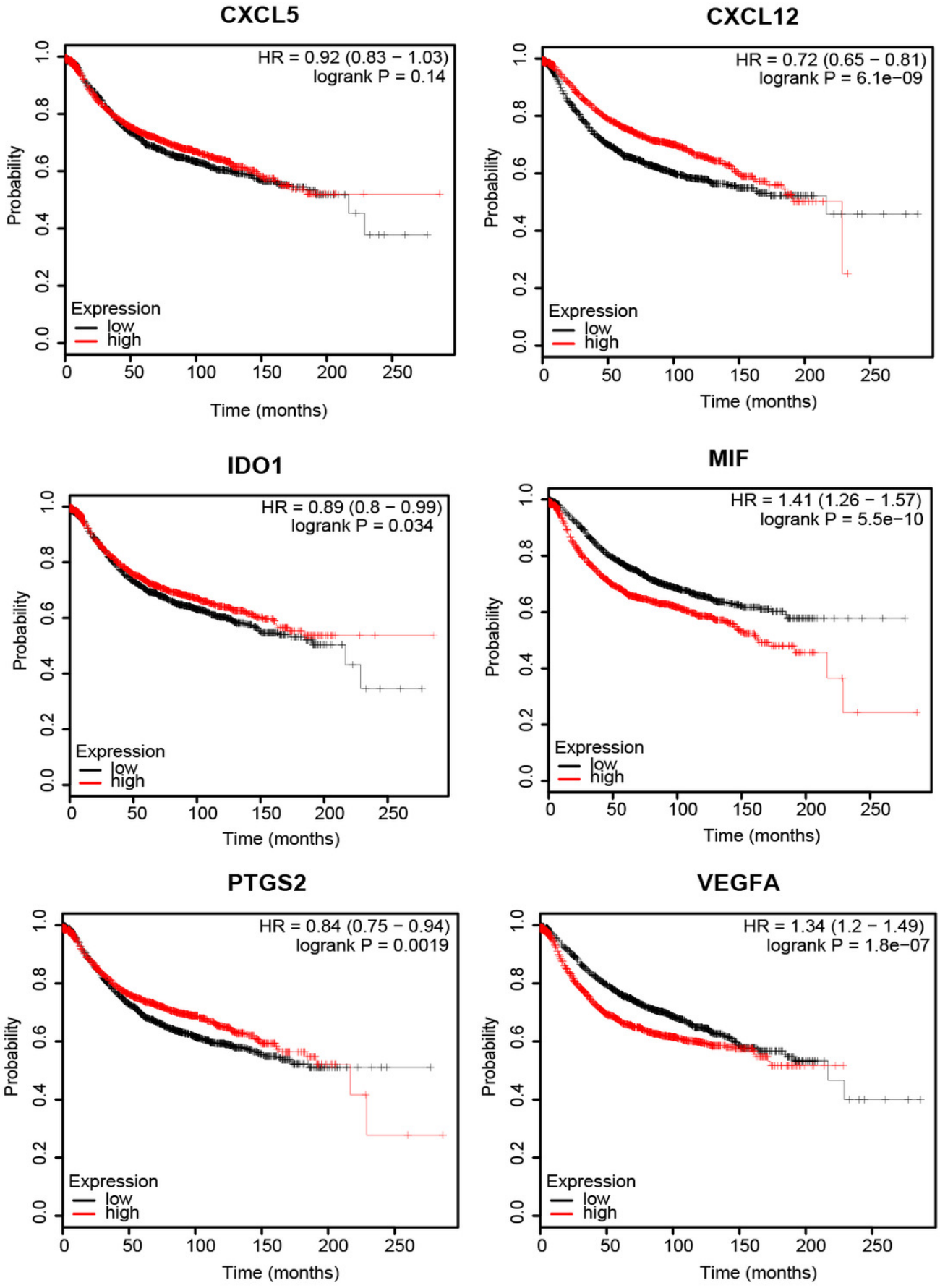
CXCL5
HR = 0.92 (0.83 − 1.03)
logrank P = 0.14
CXCL12
HR = 0.72 (0.65 − 0.81)
logrank P = 6.1e−09
IDO1
HR = 0.89 (0.8 − 0.99)
logrank P = 0.034
MIF
HR = 1.41 (1.26 − 1.57)
logrank P = 5.5e−10
PTGS2
HR = 0.84 (0.75 − 0.94)
logrank P = 0.0019
VEGFA
HR = 1.34 (1.2 − 1.49)
logrank P = 1.8e−07
Probability
Time (months)
Expression
low
high

Figure 7

Immunohistochemical detection of MIF (Row 1) and VEGFA (Row 2) in breast cancer tissue microarray.

(A) and (D), Negative expression in Cancer adjacent normal breast tissue. (B) and (E), Negative expression in Invasive ductal carcinoma. (C) and (F), Positive expression in Invasive ductal carcinoma. (Original magnification × 200; inset × 400)

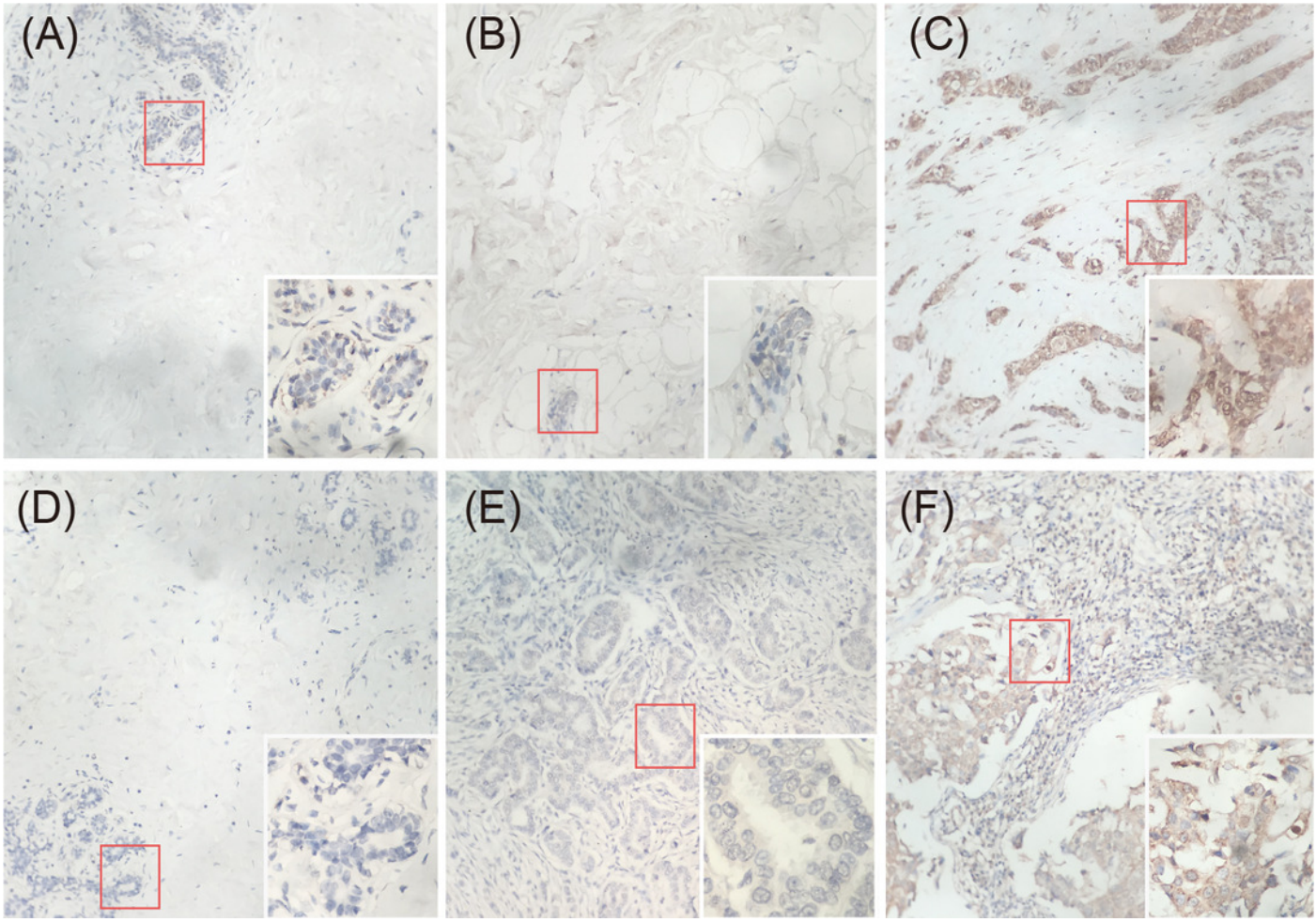

Figure 8

qRT-PCR and Western blot results.

(A) show that CD274 and IL8 were upregulated in the basal-like breast cancer cell lines, BT549 and MDA-MB-231 ($p<0.0001$). Similar to qRT-PCR results, western blot analysis (B) indicates that CD274 and IL8 protein were increased in BT549 and MDA-MB-231, compared to MCF7 and T47D cell lines. ***P<0.001, **P<0.01, *P<0.05

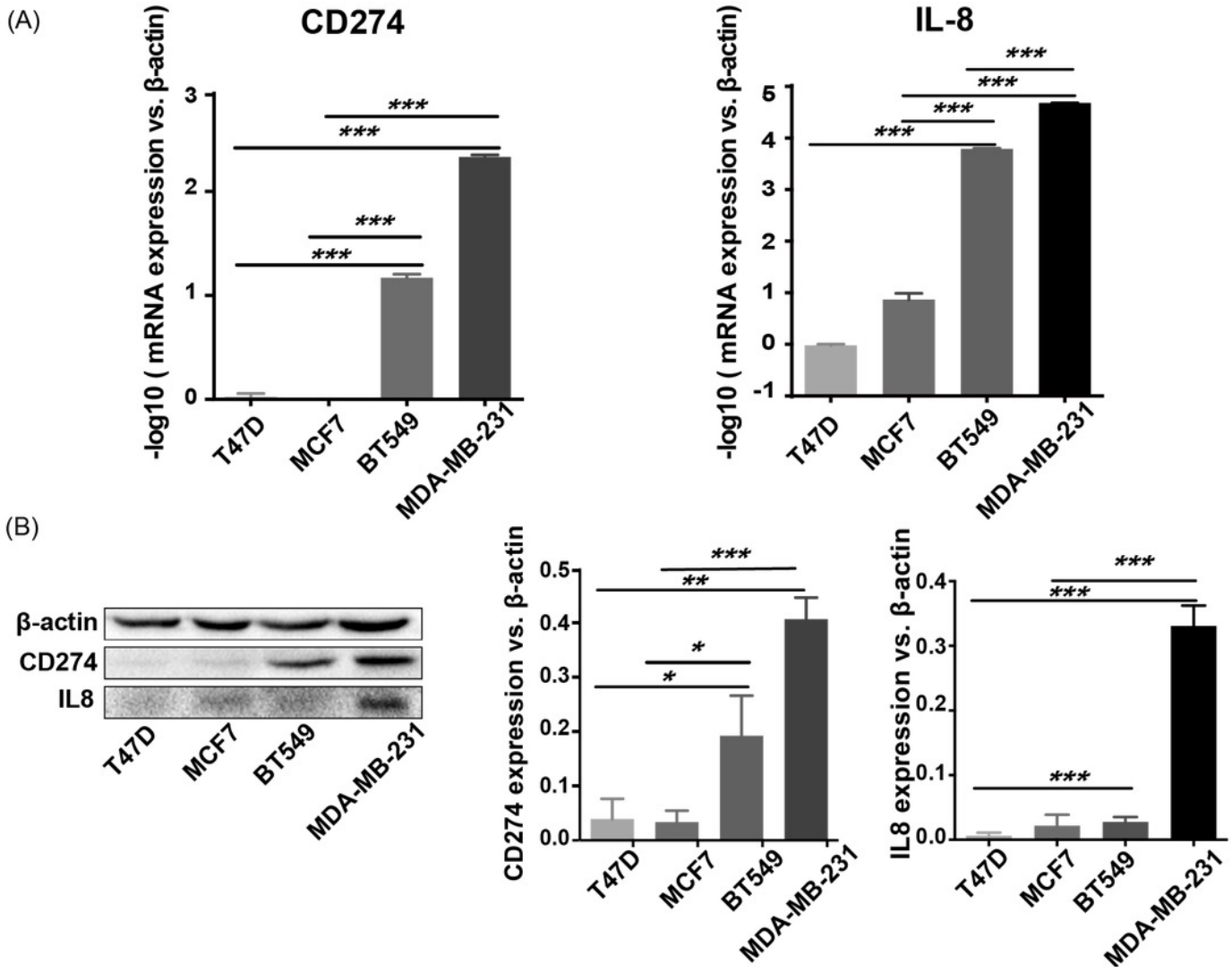

Table 1(on next page)

TOP 10 GO terms of GO functional annotations for genes in module black

Table 1. TOP 10 GO terms of GO functional annotations for genes in module black.

GO TERM_MF	Count	%	P-Value
GO:0006955~immune response	72	24.91	5.94E-53
GO:0002250~adaptive immune response	30	10.38	1.38E-23
GO:0050776~regulation of immune response	31	10.72	2.30E-22
GO:0060333~interferon-gamma-mediated signaling pathway	20	6.92	1.40E-18
GO:0006954~inflammatory response	37	12.80	4.16E-18
GO:0050852~T cell receptor signaling pathway	23	7.96	1.79E-15
GO:0045087~innate immune response	34	11.76	6.47E-14
GO:0050900~leukocyte migration	20	6.92	6.71E-14
GO:0031295~T cell costimulation	17	5.88	7.59E-14
GO:0019882~antigen processing and presentation	14	4.84	2.48E-12
GO TERM_BP			
GO:0042605~peptide antigen binding	11	3.81	6.26E-12
GO:0004888~transmembrane signaling receptor activity	18	6.23	3.51E-08
GO:0004872~receptor activity	18	6.23	4.30E-08
GO:0008009~chemokine activity	10	3.46	4.93E-08
GO:0032395~MHC class II receptor activity	7	2.42	5.49E-08
GO:0005102~receptor binding	22	7.61	1.30E-07
GO:0042288~MHC class I protein binding	7	2.42	2.83E-07
GO:0019864~IgG binding	6	2.08	3.50E-07
GO:0023026~MHC class II protein complex binding	6	2.08	3.11E-06
GO:0003823~antigen binding	11	3.81	4.10E-06

Note: GO, gene ontology; BP, biological process; MF, molecular function.

Table 2(on next page)

TOP 10 clusters of KEGG pathway enrichment analysis for genes in module black

Table 2. TOP 10 clusters of KEGG pathway enrichment analysis for genes in module black

KEGG_PATHWAY	Count	%	P-Value
hsa05330:Allograft rejection	19	6.57	9.37E-20
hsa04612:Antigen processing and presentation	24	8.30	2.51E-19
hsa05332:Graft-versus-host disease	18	6.23	2.87E-19
hsa05416:Viral myocarditis	20	6.92	5.00E-17
hsa04940:Type I diabetes mellitus	18	6.23	5.08E-17
hsa05150:Staphylococcus aureus infection	19	6.57	3.46E-16
hsa05320:Autoimmune thyroid disease	18	6.23	3.69E-15
hsa05152:Tuberculosis	27	9.34	2.08E-13
hsa04145:Phagosome	25	8.65	2.78E-13
hsa04514:Cell adhesion molecules (CAMs)	24	8.30	6.94E-13

Table 3(on next page)

Relationship between MIF, VEGFA expression level and clinico-pathologic parameters of breast cancer by tissue microarray

Table3. Relationship between MIF, VEGFA expression level and clinico-pathologic parameters of breast cancer by tissue microarray

Variable	Number of cases	MIF, 100%		P	VEGFA, 100%		P
		High	Low		High	Low	
Pathologic grade							
1	16	11 (68.8)	5 (31.2)	0.397	6 (37.5)	10 (62.5)	0.017*
2,3	58	32 (55.2)	26 (44.8)		42 (72.4)	16 (27.6)	
Clinical stage							
I	17	3 (17.6)	14 (82.4)	0.095	12 (70.6)	5 (29.4)	1.000
II, III	73	30 (41.1)	43 (58.9)		51 (69.9)	22 (30.1)	
Lymph node status							
No metastasis	78	25 (32.1)	53 (67.9)	0.027*	48 (61.5)	30 (38.5)	0.524
Metastasis	12	8 (66.7)	4 (33.3)		9 (75.0)	3 (25.0)	

The total number of samples in pathologic grade does not equal 90, as some samples are not included in any given grades. * $p<0.05$